Hierarchical Self-Assembly and Conformation of Tb Double-Decker Molecular Magnets: Experiment and Molecular Dynamics

Patrick Lawes, Mauro Boero, Rabei Barhoumi, Svetlana Klyatskaya, Mario Ruben, Jean-Pierre Bucher

Hierarchical self-assembly and conformation of Tb double-decker molecular magnets: experiment and molecular dynamics.

P. Lawes[1,2], M. Boero[1], R. Barhoumi[1,2], S. Klyatskaya[2], M. Ruben[2], and J.P. Bucher[1]*

[1] Université de Strasbourg, IPCMS UMR 7504, F-67034 Strasbourg, France.
[2] Karlsruher Institut für Technologie, Institut für Nanotechnologie, D-76344 Eggenstein-Leopoldshafen, Germany

Keywords: 2D Self-Assembly, Molecular Magnets, Bis(phthalocyaninato)Terbium, STM, Molecular Dynamics, Conformation, Double-Decker

Abstract: *Nanostructures, fabricated by locating molecular building-blocks in well-defined positions, for example on a lattice, are ideal platforms for studying atomic-scale quantum effects. In this context, STM data of self-assembled $TbPc_2$ single molecule magnets on various substrates have raised questions about the conformation of the $TbPc_2$ molecules within the lattice. In order to address this issue, molecular dynamics simulations were carried out on a 2D assembly of $TbPc_2$ molecules. The calculations are in excellent agreement with the experiment, and thus improve our understanding of the self-assembly process. In particular, the calculated electron density of the molecular assembly compares well with STM contrast of self-assembled $TbPc_2$ on Au(111). It is found that it is not necessary to consider a dihedral angle different from 45° between the two Pc ligands of the double-decker molecule to account for the experimental result. Furthermore, the relatively strong molecule-molecule interaction in small islands of a few molecules is progressively weakened when the 2D lattice is formed due to multiple interaction with surrounding molecules.*

1.Introduction

Single molecule magnets (SMMs) have been the object of intense research due to their potential application in magnetic data storage, molecular spintronics and as qubits for quantum computation [1]. However, the use of single molecules requires their proper organization on a surface as a prerequisite to control their individual addressing for example by means of the tip of an STM [2]. This is a key issue since intermolecular interactions and molecule-substrate interactions play an important role on the properties of a monolayer. Part of these properties can be tuned by implementing proper functional groups. Conformation can change as a result of these interactions, thus impacting on the spin properties of the SMMs. In this context, the lanthanide double-decker complexes were found to exhibit interesting SMM behavior at low temperatures [3-10], without exhibiting the disadvantages of some other systems [11]. The double-decker complexes involving the phthalocyanine sandwich approach have been extensively investigated, and (as a matter of fact) significant breakthroughs recorded in the field of molecular magnets are lanthanide-based, mostly attributed to the large anisotropy arising from the unquenched orbital angular momentum of the f−orbitals.

Due to their spin properties, the lanthanide double-decker molecules gained most relevance in the realization of the qubits for quantum information processing (QIP) [12-14].

Developments have accelerated when a reliable electric readout of the quantum information of a single-spin qubits was proposed. In this context the bis(phthalocyaninato Tb(III) ($TbPc_2$) single molecule magnet, is one of the well-known examples in which the delocalized π-radical electron spin of the Pc ligand allows the reading of electronic and nuclear spin state of the Tb qubits [15,16]. It has been evidenced that the π-radicals also play a major role in the quantum mechanical associations of such SMM's [6].

Structurally, $TbPc_2$ features a central Tb^{3+} octa-coordinated ion sandwiched between two parallel phthalocyanines, with a dihedral rotation angle between the Pc-ligands close to ϑ= 45°, leading to a square-antiprismatic (D_{4d}) coordination geometry [3,4] (see Figure 1). Whereas the dihedral angle of 45° is adopted by the stable gas-phase molecules it is also the usual conformation for isolated molecules on surfaces [5,6,17]. However, from a series of STM measurements on monolayers of lanthanide double-deckers ($LnPc_2$) on surfaces, it was inferred that the molecules can also adopt a ϑ= 30° dihedral angle (or some other values different from 45°) [5-8], leading for example to a square checkerboard arrangement of 45° and 30° molecules. The reasoning was as follows: It was assumed that the lower Pc ligands, those in contact with the substrate, all adopt the same orientation, similar to the ones observed in single metalo-phthalocyanine monolayers [18]. Since the upper Pc's of the double-decker adopt different orientations inside of the molecular layer (STM observation), it was then necessary to postulate the existence of at least two conformations with different dihedral angles for the molecules constituting the layer.

However, these conclusions came only as a best guess and were not based on any direct observations since only the top Pc ligand is "visible" in STM experiments. As a result, this assumption has never been verified properly. It is noteworthy that other works on monolayer of $LnPc_2$ did not claim such an alternation in the dihedral angle [6,8,9,10]. In particular, it has been found that 2D islands made of a small number of $TbPc_2$ molecules (one to four) on Au(111) follow well-defined, arrangement with ϑ= 45° that optimizes compactness [6]. It is the purpose of this work to find out to what extent the association of molecules in networks can modify their conformation and hence their electronic and magnetic properties.

2. Materials and Methods

Scanning tunneling microscopy and spectroscopy

All sample preparations were carried out in an ultrahigh vacuum (UHV) system with a base pressure of 1 x 10^{-10} mbar. The single crystalline of Au(111) substrate were cleaned by Ne^+ sputtering and annealing cycles. The powder sample of $TbPc_2$ molecules (synthesized by the Ruben group at the Karlsruhe Institute of Technology) was first degassed *in-vacuo*, at a temperature slightly below the sublimation temperature for several hours. Deposition of $TbPc_2$ occurred at a sublimation temperature of 600 K onto the substrates kept at room temperature. Molecule sublimation was performed in a side chamber of the UHV system; during this operation the pressure was kept below 1 x 10^{-9} mbar. All STM/STS data were acquired at 4.5 K. STS spectra were measured using a lock-in detection with a modulation between 1 mV and 10 mV (rms) depending on the features to be resolved. Manipulation by means of the STM tip of this category of molecules was described earlier [17-19].

Computational method

We resort to first principles simulations within the density functional theory[43] (DFT) framework as implemented in the CPMD[44] code. The Becke exchange[45] and the Lee-Yang-Parr correlation[46] functional have been used to describe the exchange and correlation contributions, complemented by the exact exchange[47] (B3LYP). Core-valence interactions have been described by norm-conserving Troullier-Martins[48] pseudopotentials (PPs) for N, C, and H, while for Tb we make use of a Goedecker-Teter-Hutter[49] semicore PP. Valence electron orbitals were represented in a plane wave (PW) basis set with a cut-off energy of 80 Ry. To eliminated the problem of periodically repeated images, typical of standard PW approaches, an isolated cell[50] with an edge of 47.7 Å was used. A spin-unrestricted approach is adopted in all the simulations and van der Waals interactions were included according to Grimme's D2 formula.[51] All structures have been fully optimized until residual atomic forces are smaller than 10^{-4} Hartree/Bohr.

-First principles simulations within the density functional theory (DFT) framework + vdW Grimme D2.
-Becke exchange & Lee-Yang-Parr correlation functional complemented by the exact exchange (B3LYP).
-Core-valence interactions described by norm-conserving Troullier-Martins pseudopotentials (PPs) for N, C, and H and for Goedecker-Teter-Hutter semicore PP for Tb.
-Valence electron orbitals represented in a plane wave (PW) basis set with a cut-off energy of 80 Ry.
-Isolated cubic simulation cell (Phys. Rev. B **1993**, *48*, 2081) with a side of 47.7 Å.

3. Results and discussion

In a previous work, it was found that interactions between molecules in a cluster are such that only two types of molecular building blocks are found corresponding to the parallel (dimer in Figure 2a) and staggered (see the trimer in Figure 2b) packing of the molecules. In either case it has been unambiguously determined that each $TbPc_2$ molecule conserves it $\vartheta = 45°$ dihedral-angle (for details, see Ref. [6]). Additionally, the quantum mechanical behavior of molecular π-radicals in the cluster formation has been emphasized and detected by the Kondo resonance measurement with atomic resolution. With increasing island size, however, molecules have to accommodate multiple interactions and therefore adopt a more complex geometrical arrangement such as observed by STM on semi-infinite 2D domain (lower left of Figure 2a and b and Figure 2c) whose understanding is the main purpose of the present work.

The square checkerboard lattice mentioned above for monolayers of $TbPc_2$ molecules on Au(111) manifests itself by alternating bright and dark STM contrasts located in the center part of the molecules, see Figure 2 [5-7]. Here we just call them A and B respectively (Figure 2c). It was observed however that these contrasts only appear at specific values of the bias voltage [7], referring to a possible spectroscopic origin. For example, the STM image of Figure 2c has been acquired at -0.5 V and shows contrasts that are in good agreement with those observed by others on the same system and in the same bias voltage interval [5]. In addition, the HOMO-LUMO gap measured at 760 meV for a single $TbPc_2$ molecule on Au(111) [6] is now strongly decreased as shown on spectra acquired above the 2D molecular lattice (Figure 2d). The HOMO-LUMO gap is only 100 and 200 meV (vertical arrows) for A and B molecules

respectively. The reduction in the gap is due to the molecular orbital overlap induced by the 2D lattice formation. However, at this stage, and in the absence of specific hints, it remains impossible to identify unequivocally the origin of the STM contrast. One should add that, to date, no calculation was able to fully explain the origin of A and B contrasts observed in STM experiments. The difficulty comes from the large number of atoms to be considered in the unit cell of a semi-infinite system. In this work we address this issue by mean of a full molecular dynamics and ab-initio DFT calculation, taking into account the symmetry of the system and the weak interaction observed between the $TbPc_2$ molecules and the Au(111) substrate.

For the geometrical optimization we initiate the calculation with an assembly of four $TbPc_2$ molecules with a dihedral angle of 45° (see Figure 3a). The only experimental input is the dimension of the square lattice (1.42 nm). Periodic boundary conditions are adopted for the calculation. For the optimization of the molecular dynamics process we consider that the molecule substrate interaction can be neglected in first approximation based on the mobility of compact clusters such as tetramers on Au(111) tested by means of the STM manipulation [6]. This approach is validated by the stability of the molecules radical on Au(111) as probed by the Kondo physics (absence of charge transfer from the substrate). After full relaxation of the system, it is found that the tetramer keeps its quasi flat 2D configuration (Figure S1) and above all, the dihedral angles of all molecules remain unchanged, and equal to 45° (Figure 3a). In addition, it is found that the molecules adopt two different azimuthal orientations for A and B. The A and B orientations are found along either diagonal of the square lattice (see Figure 3a). Simulation was initiated from other configurations but always converged to the one shown in Figure 3a with 45° dihedral angle for both, A and B sites.

For comparison with the STM experiment, Figure 3b shows the calculated electron density within an interval [E_F - 0.5 eV, E_F]. It can be noted that the external lobes correspond well with the STM image of Figure 2c. The agreement with the experiment also holds for the molecular orbital overlap between two adjacent molecules, highlighted by the circle in the electron density image of Figure 3b. In addition to the eight external lobes of the upper Pc, the electron density of Figure 4 clearly shows that eight small, inner lobes merge into a cross-like contrasts. These results compare well with the experiment for data taken within the same energy range of the applied sample bias [6]. The results reflect the checkerboard symmetry of the system in that A-type molecules exhibit one azimuthal orientation whereas B-type molecules exhibit another azimuthal orientation. From the inner lobes contrast it is easily found that the whole B molecule is rotate by 30° clockwise with respect to the A molecule in perfect agreement with the experiment [6].

It is instructive to consider the images obtained for different values of the electron density. It is found that the correspondence with the STM experiment is better for low density values such as 1 x 10^{-5} e/Å^3 (Figure 3b) as opposed to 1 x 10^{-4} e/Å^3 or 1 x 10^{-2} e/Å^3 (Figure S3) which makes sense, since the STM experiment accesses primarily the tail of the wave function. The energy range explored by the STM experiment is also decisive, typically between E_F - 0.5 eV and E_F since a larger interval (involving deeper energy levels) leads to a significantly different picture (Figure S3b).

An energy level analysis close to the Fermi energy sheds additional light on the properties of the molecular arrangement (see Figure 4a). As expected, the HOMO-LUMO gap of the so

assembled molecules is decreased from the single molecule to less than 200 meV in good agreement with the experiment (see Figure 2d). Let us now consider the HOMO and HOMO-1 states relevant for the STM spectroscopy analysis. According to Figure 4b,c we find that both spin orientations of the HOMO localize on A-type molecules, whereas both spin directions of the HOMO-1 localize on the B-type molecules. The fact that the HOMO wave function is found exclusively on A-molecules and the HOMO-1 wave function exclusively on B-molecules is an additional confirmation of the electronic (spectroscopic) origin of the checkerboard symmetry observed in the STM contrasts.

4. Conclusions

The very good agreement of the calculation with the experiment tells us that there is no need to consider two sets of conformationally different molecules, as proposed previously. It is found that the molecules are able to arrange so as exhibit the same alternating contrast observed experimentally and simultaneously leading to a ϑ = 45° dihedral angle on each molecule of the assembly. Therefore, although we cannot exclude completely a small deviation (less than 2°) of the dihedral angle from 45°, we demonstrate here that the presence of a second specie with ϑ = 30° is not a necessary condition to explain the experimental observation. It is noteworthy that the good agreement between simulation and experiment is found for the low electron density calculation and the relatively narrow energy window at E_F, proof that only the tail of the wave function is captured in an STM image. In summary, this is the first time that a one to one correspondence can be established between the subtle STM contrast of $LnPc_2$ layers and the conformational arrangement of individual molecules.

Funding: P. L. acknowledges financial support from the European Union's Framework Program for Research and Innovation, Horizon 2020, under the Marie Sklodowska-Curie Grant Agreement No. 847471 (QUSTEC). M. B. thanks the HPC Mesocenter (Equip@Meso) at the University of Strasbourg, and the Grand Equipement National de Calcul Intensif (GENCI) under allocation DARI-A6 A0060906092.

References:

1) Gabarro-Riera, G.; Aromi, G.; Sanudo, E.C. Magnetic molecules on surfaces: SMMs and beyond. *Coordination Chemistry Reviews* **2023**, *475*, 214858.

2) Bogani, L.; Wernsdorfer, W. Molecular spintronics using single-molecule magnets. *Nat Mater*. **2008**, 7, 179–186.

3) Koike, N.; Uekusa, H.; Ohashi, Y.; Harnoode, C.; Kitamura, F.; Ohsaka, T.; Tokuda, K. Relationship between the Skew Angle and Interplanar Distance in Four Bis(phthalocyaninato)lanthanide(III) Tetrabutylammonium Salts ($[NBu^n_4][Ln^{III}Pc_2]$; Ln = Nd, Gd, Ho, Lu). *Inorg. Chem.* **1996**, *35*, 5798.

4) Ishikawa, N.; Sugita, M.; Ishikawa, T.; Koshihara, S.-Y.; Kaizu, Y. Lanthanide double-decker complexes functioning as magnets at the single-molecular level. *J. Am. Chem. Soc*. **2003**, *125*, 8694–8695.

5) Komeda, T.; Isshiki, H.; Liu, J.; Zhang, Y. F.; Lorente, N.; Katoh, K.; Breedlove, B. K.; Yamashita, M. Observation of Electric Current Control of a Local Spin in a Single-Molecule Magnet. *Nat. Commun*. **2011**, *2*, 217.

6) Amokrane, A.; Klyatskaya, S.; Boero, M.; Ruben, M.; Bucher J. P. The Role of π-Radicals in the Spin Connectivity of Clusters and Networks of Tb Double-Decker Single Molecule Magnets. *ACS Nano* **2017**, *11*, 10750-10760.

7) Ara, F.; Qi, Z.K.; Hou, J.; Komeda, T.; Katoha, K.; Yamashita, M. A Scanning Tunneling Microscopy Study of the Electronic and Spin States of Bis(phthalocyaninato) terbium(III) ($TbPc_2$) Molecules on Ag(111). *Dalton Trans*. **2016**, *45*, 16644-16652.

8) Katoh, K.; Komeda, T.; Yamashita, M. Surface Morphologies, Electronic Structures, and Kondo Effect of Lanthanide(III)-Phthalocyanine Molecules on Au(111) by Using STM, STS and FET Properties for Next Generation Devices. *Dalton Trans*., **2010**, *39*, 4708-4723.

9) Deng, Z.; Rauschenbach, S.; Stepanov, S.; Klyatskaya, S.; Ruben, M.; Kern, K. Self-assembly of bis(phthalocyaninato)terbium on metal surfaces. *Phys. Scr*. **2015**, *90*, 098003.

10) Gonidec, M.; Biagi, R.; Corradini, V.; Moro, F.; De Renzi, V.; del Pennino, U.; Summa, D.; Muccioli, L.; Zannoni, C.; Amabilino, D. B.; Veciana, J. *J. Am. Chem. Soc.* **2011,** *133,* 6603–6612. doi:10.1021/ja109296c

11) Rogez, G.; Donnio, B.; Terazzi, E.; Gallani, J.-L.; Kappler, J.-P.; Bucher, J.-P.; Drillon, M. The Quest for Nanoscale Magnets: The example of [Mn_{12}] Single Molecule Magnets. *Adv. Mater*. **2009**, *21*, 4323-4333.

12) Godfrin, C. ; Ferhat, A. ; Ballou, R. ; Klyatskaya, S. ; Ruben M. ; Wernsdorfer, W. ; Balestro, F. Operating quantum states in single magnetic molecules: implementation of Grover's quantum algorithm. *Phys. Rev. Lett*. **2017**, *119*, 187702.

13) Wernsdorfer, W.; Ruben, M. Synthetic Hilbert Space Engineering of Molecular Qudits: Isotopologue Chemistry. Mater. **2019**, *31*, 1806687. https://doi.org/10.1002/adma.201806687

14) Gaita-Ariño, A. ; Luis, F. ; Hill, S. ; Coronado, E. Molecular spins for quantum computation. *Nat. Chem*. **2019**, *11*, 301–309. https://doi.org/10.1038/s41557-019-0232-y

15) Vincent, R.; Klyatskaya, S.; Ruben, M.; Wernsdorfer, W.; Balestro, F. Electronic Read-Out of a Single Nuclear Spin Using a Molecular Spin Transistor, *Nature*, **2012**, 488, 357–359.

16) Urdampilleta, M.; Klayatskaya, S.; Ruben, M.; Wernsdorfer, W. Magnetic Interaction Between a Radical Spin and a Single-Molecule Magnet in a Spin Valve. *ACS Nano* **2015**, 9, 4458– 4464.

17) Barhoumi, R.; Amokrane, A.; Klyatskaya, S.; Boero, M.; Ruben, M.; Bucher, J.P. Screening the 4f-electron spin of $TbPc_2$ single-molecule magnets on metal substrates by ligand channeling. *Nanoscale* **2019**, *11*, 21167.

18) Tuerhong, R.; Ngassam,F.; Watanabe, S.; Onoe, J.; Alouani, M.; Bucher, J.P. Two-Dimensional Organometallic Kondo Lattice with Long-Range Antiferromagnetic Order. *J. Phys. Chem*. **2018**, *122*, 20046.

19) Tuerhong, R.; Ngassam, F.; Alouani, M.; Bucher, J.P. When Molecular Dimerization Induces Magnetic Bi-Stability at the Metal–Organic Interface. *Adv. Phys. Res*. **2023**, 2: 2200005. https://doi.org/10.1002/apxr.202200005

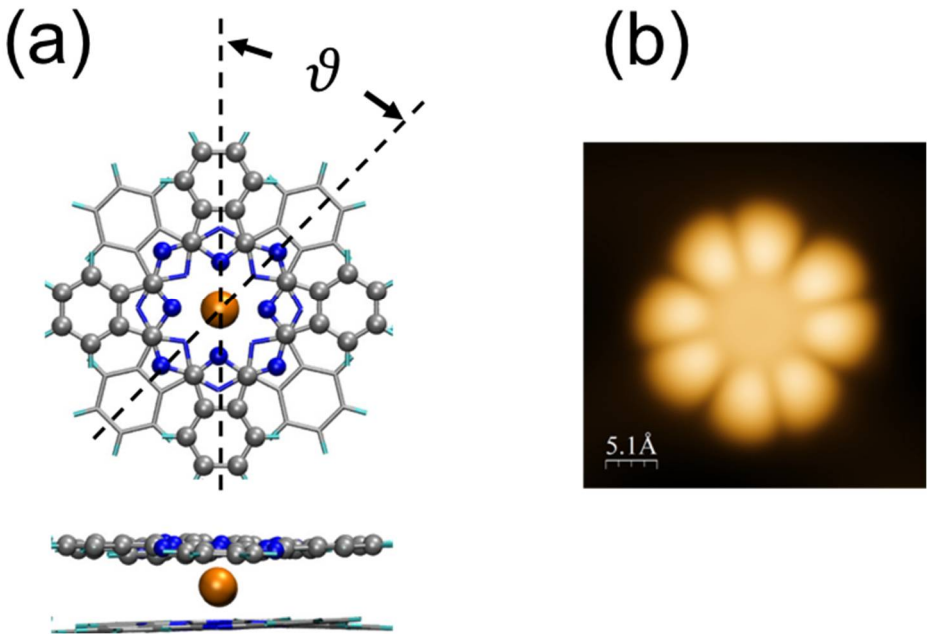

Figure 1. (a) Geometry of the TbPc2 molecule. ϑ is the dihedral angle between the upper Pc (balls) and the lower Pc (sticks). Color code: C (grey), N (blue), Tb (orange). (b) STM image (60 pA , −0.3 V) of a single $TbPc_2$ molecule on Au(111), only the upper Pc is visualized by STM.

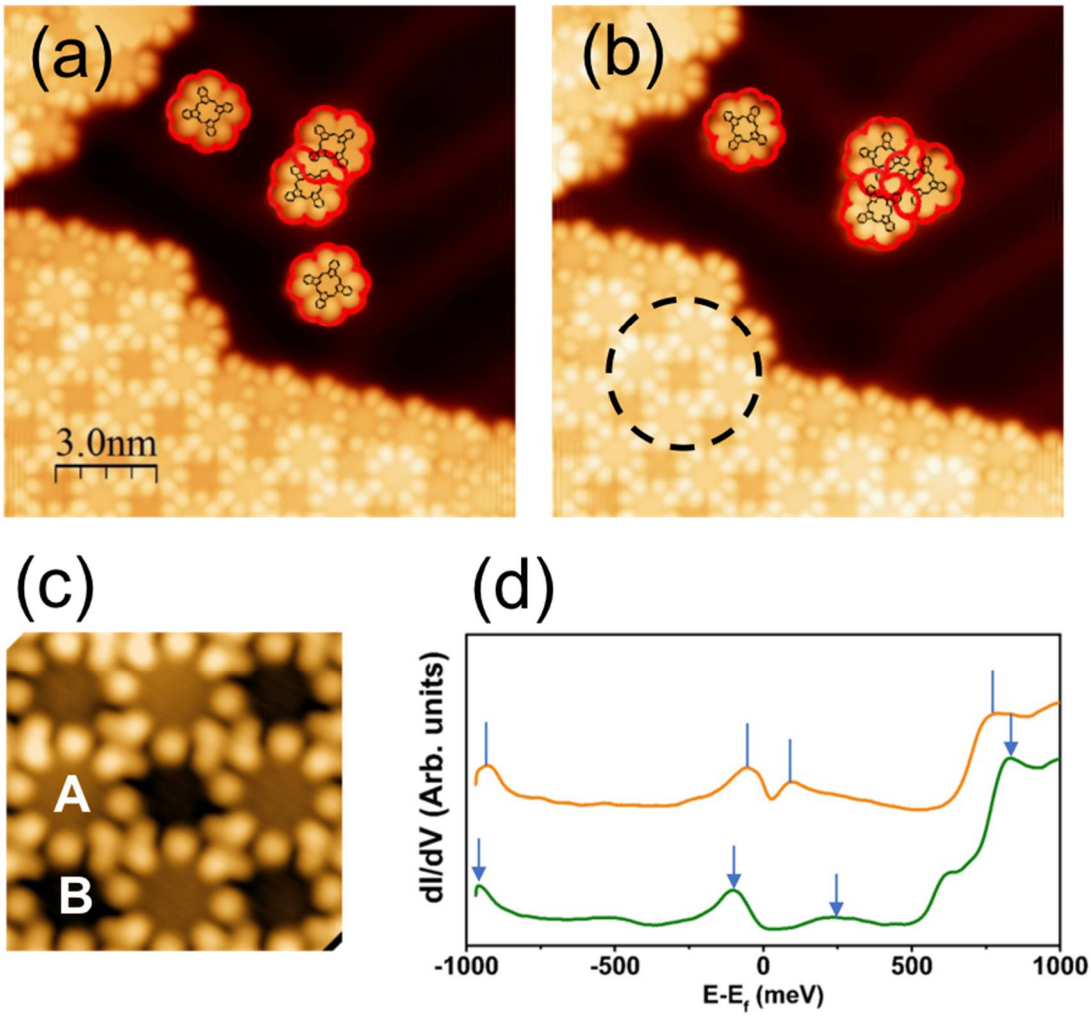

Figure 2. (a, b) Constant current STM images (70 pA, −0.3 V) of $TbPc_2$ molecular islands and clusters grown on Au(111). Contours of upper Pc's are highlighted in red. (c) Zoom-in image of the circled area in (b) showing bright (A) and dark (B) contrasts for molecules in a domain (70 pA, −0.3 V). (d) dI/dV spectroscopy performed at the center of A-type (red) and B-type (black) molecules respectively. Vertical lines/arrows show the correspondence between different peaks. Figures a) and b) from ref [6] with permission. Further permissions related to the material excerpted should be directed to the ACS.

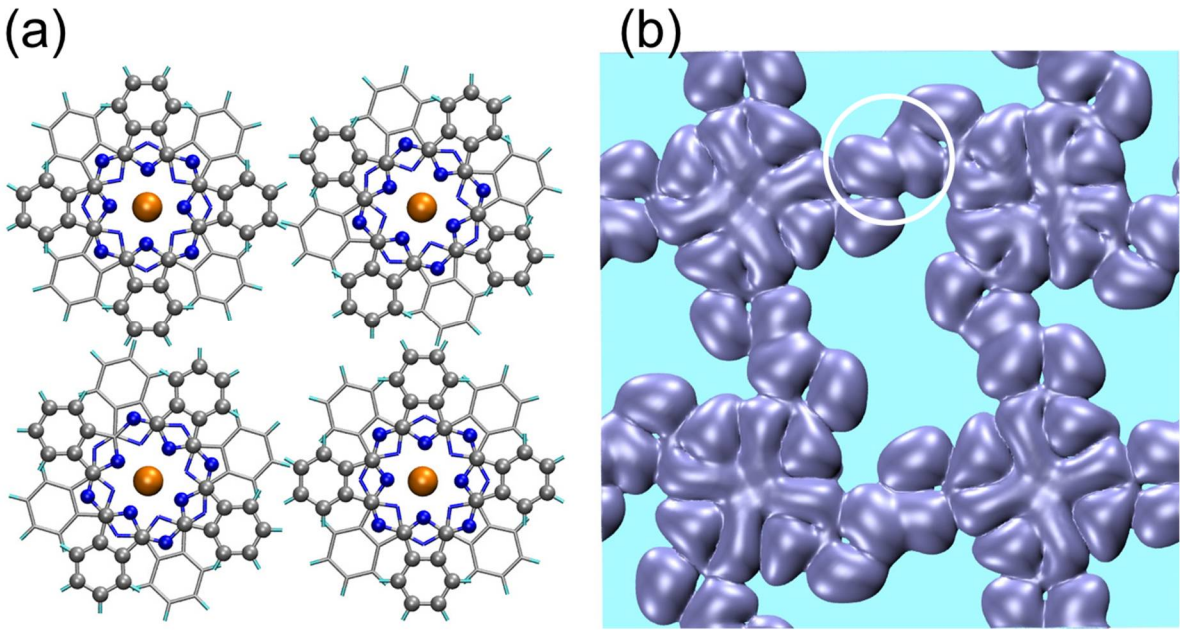

Figure 3. (a) Primitive cell 1 x 1 of an assembly of four $TbPc_2$ molecules with periodic boundary conditions. Balls, upper-Pc and sticks, lower-Pc. Color code: C (grey), N (blue), Tb (orange). The only experimental input is the dimension of the square lattice (1.42 nm). After full relaxation, it is found that the dihedral angle $\vartheta = 45°$ for all the molecules and remains unchanged, independent of initial configuration. (b) Electron density 1 x 10^{-5} e/Å^3 in the range [E_F - 0.6 ,E_F] eV, top view, above the upper Pc. The circle indicates the molecular orbital overlap between adjacent molecules.

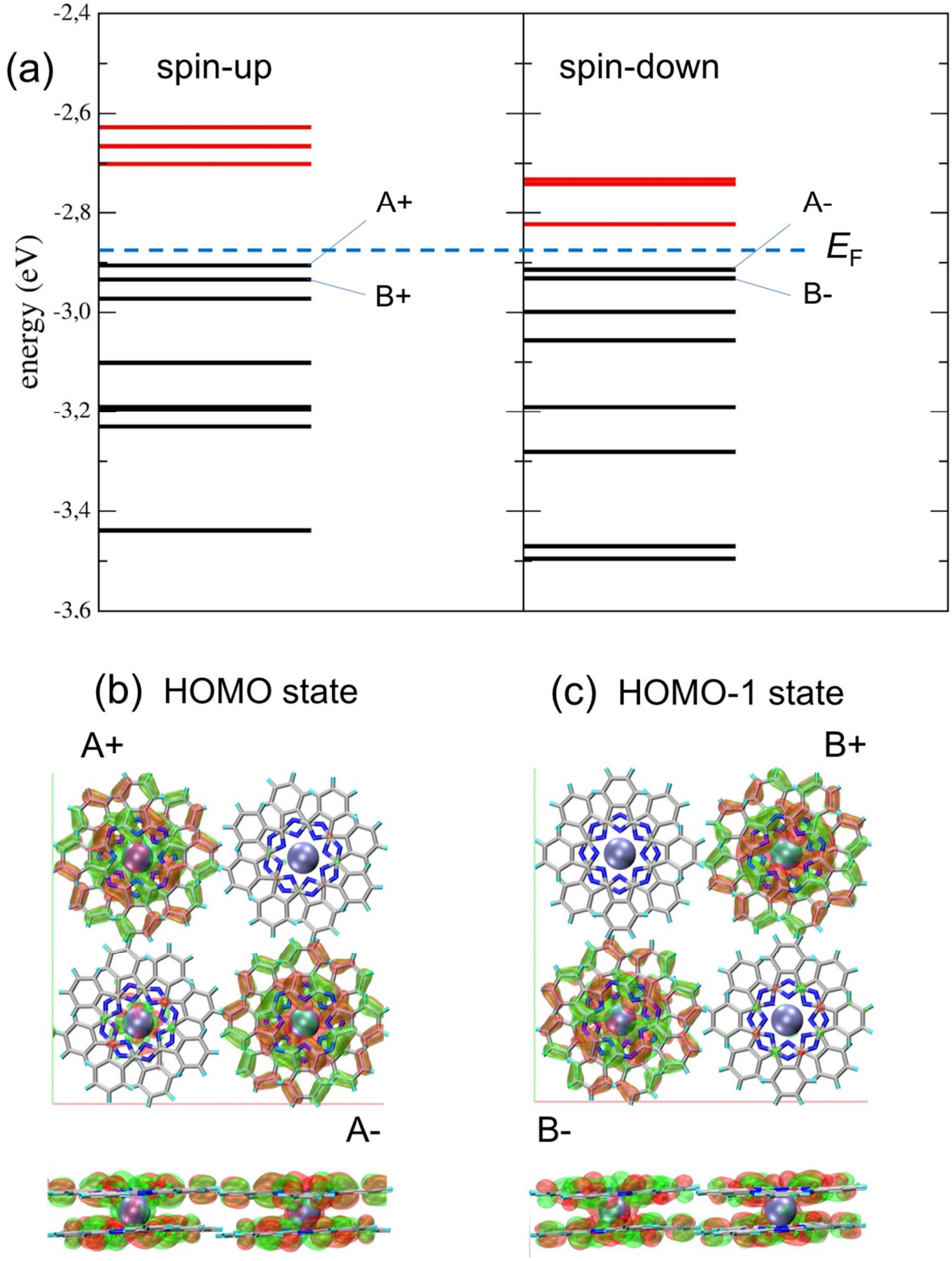

Figure 4. (a) Distribution of energy levels close to the Fermi energy (doted blue line). The levels are labeled A and B to refer to the location of the corresponding wave function with spin up (+) and spin down (-). (b,c) Top- and side-views of HOMO and HOMO-1 wave functions respectively. The HOMO-1 state is -0.03 eV below HOMO. Molecule labeling corresponds to the energy levels in (a).